Analysis of Entropy Generation in a Generalized Couette Flow between Two Concentric Pipes with Buoyancy Effect

A. S. Eegunjobi[1], O. D. Makinde[2] and A. P. Oluwagunwa[3,*]

[1]*Department of Mathematics and Statistics, Namibia University of Science and Technology, Private Bag 13388, 13 Storch Street, Windhoek, Namibia*

[2]*Faculty of Military Science, Stellenbosch University, Private Bag X2, Saldanha 7395, South Africa*

[3]*Department of Mathematics and Statistics, Rufus Giwa Polytechnic, Owo, Ondo State, Nigeria*

Abstract: Heat transfer and entropy generation analysis in buoyancy driven generalized Couette flow of variable viscosity fluid within the annulus of two concentric cylindrical pipes are theoretically investigated. It is assumed that the inner cylinder is fixed while the outer one is subjected to axial motion. The governing nonlinear equation models are obtained and solved numerically using shooting quadrature. The results for velocity and temperature profiles are utilized to compute entropy generation number and the Bejan number. Relevant results are displayed graphically and discussed quantitatively.

Keywords: Generalized couette flow, concentric pipe annulus, variable viscosity, bouyancy force, heat transfer, entropy generation.

1. INTRODUCTION

Couette flows occur either between two parallel flat plates or between concentric cylinders. Generalized Couette flow differs from couette flow due to the fact that pressure gradient is superimpose in the direction of the flow. These flows have many significance applications in engineering and industries such as MHD pumps, MHD generators, accelerators, flow meters and nuclear reactors, journal bearing, aerodynamic heating and metal extrusion. Makinde and Franks [1] investigated the effect of magnetic field on a reactive unsteady generalized couette flow with temperature dependent viscosity and thermal conductivity. Attia and Sayed-Ahmed [2] studied the unsteady MHD flow of an electrical conducting viscous incompressible non-Newtonian ocasson fluid bounded by two parallel non-conducting porous plates with heat transfer putting into consideration the Hall effects.

Theuri and Makinde [3] conducted an analysis of the first and second law of thermodynamics on a temperature dependent viscosity hydromagnetic generalized unsteady Couette flow with permeable walls. Asghara and Ahmada [4] constructed the analytic solution for unsteady Couette flow in the presence of an arbitrary non-uniform applied magnetic field. Chinyoka and Makinde [5] investigated the transient problem of generalized Couette flow and heat transfer in a reactive variable viscosity third grade liquid with asymmetric convective cooling. Eegunjobi and Makinde [6] numerically investigated the entropy generation rate in a transient variable viscosity Couette flow between two concentric pipes. A list of the key references in the vast literatures concerning Couette flow and generalized Couette flow are given in references [7-11].

In this paper, we consider the irreversibility analysis in a generalized Couette flow within the annulus of concentric pipes with buoyancy effect and variable viscosity. In the flow, the outer cylinder moves in the axial direction while the inner cylinder remains fixed. Mathematical formulation of the problem is given in section two while the entropy generation analysis is presented in section three. The models boundary value problem are tackled numerically using shooting quadrature coupled with Runge-Kutta-Fehlberg integration scheme. Relevant results are presented graphically and discussed quantitatively for velocity, temperature, skin friction, Nusselt number, entropy generation rate and Bejan number.

2. MATHEMATICAL MODEL

The steady flow of an incompressible viscous fluid between two concentric cylindrical pipes separated by $r_1 - r_0$ in a generalized Couette flow with the inner cylinder stationary and the outer cylinder moving is considered in the presence of buoyancy effect as shown in Figure **1**.

*Address correspondence to this author at the Department of Mathematics and Statistics, Rufus Giwa Polytechnic, Owo, Ondo State, Nigeria;
E-mail: petergunwa@gmail.com

E-ISSN: 2409-5826/16

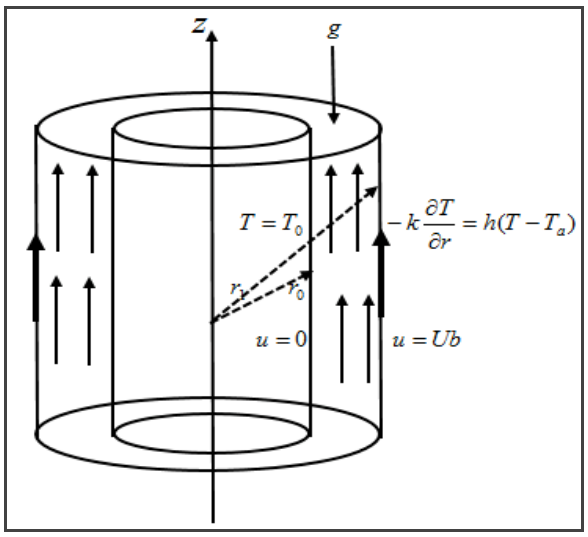

Figure 1: Geometry of the problem.

The governing equations of the motion are given as:

$$\frac{\partial u}{\partial z} = 0 \tag{1}$$

$$-\frac{\partial P}{\partial z} + \frac{1}{r}\frac{\partial}{\partial r}\left(r\mu(T)\frac{\partial u}{\partial r}\right) + g\beta\left(T - T_a\right) = 0 \tag{2}$$

$$\frac{k}{r}\frac{\partial}{\partial r}\left(r\frac{\partial T}{\partial r}\right) + \mu(T)\left(\frac{\partial u}{\partial r}\right)^2 = 0 \tag{3}$$

The boundary conditions are:

$$\left.\begin{aligned} u = 0, \quad T = T_0 \qquad & at \qquad r = r_0 \\ u = Ub, \quad -k\frac{\partial T}{\partial r} = h(T - T_a) \qquad & at \qquad r = r_1 \end{aligned}\right\} \tag{4}$$

where *u* is the axial velocity, z is the axial distance, P is the pressure, g is the acceleration due to gravity, T is the temperature, T_a is the ambient temperature, T_0 is the inner cylinder temperature, U is the mean velocity, Ub is the velocity of the outer wall, b is wall parameter or outer cylinder movement parameter, β is the volumetric expansion coefficient, h is the heat transfer coefficient, k is thermal conductivity of the material, r_0, r_1 are the inner and outer radii respectively.

The temperature dependent viscosity $\mu(T)$ can be expressed as:

$$\mu(T) = \mu_0 e^{-m\left(T - T_a\right)} \tag{5}$$

where m is a viscosity variation parameter and μ_0 is the fluid dynamic viscosity at the ambient temperature. We introduce the nondimensional quantities:

$$\left.\begin{aligned} &\theta = \frac{T - T_a}{T_0 - T_a}, w = \frac{u}{U}, \ \eta = \frac{r}{r_0}, \ \nu = \frac{\mu_0}{\rho}, \ \mathrm{Pr} = \frac{\mu_0 c_p}{k}, \ Bi = \frac{r_0 h}{k} \\ &\delta = \frac{r_1}{r_0}, \ \overline{P} = \frac{r_0 P}{U\mu_0}, \psi = -\frac{\partial \overline{P}}{\partial z}, Z = \frac{z}{r_0}, \gamma = m\left(T_0 - T_a\right) \end{aligned}\right\} \tag{6}$$

Substituting equation (6) into equations (1)–(5), we obtain the dimensionless governing equations for the momentum and energy as:

$$\psi + \frac{1}{\eta}\frac{d}{d\eta}\left(\eta e^{-\gamma\theta}\frac{dw}{d\eta}\right) + Gr\theta = 0, \tag{7}$$

$$\frac{1}{\eta}\frac{d}{d\eta}\left(\eta\frac{d\theta}{d\eta}\right) + Bre^{-\gamma\theta}\left(\frac{dw}{d\eta}\right)^2 = 0, \tag{8}$$

with the boundary conditions:

$$\left.\begin{aligned} &w(1) = 0, \theta(1) = 1, \\ &w(\delta) = b, \qquad \frac{d\theta}{d\eta}(\delta) = -Bi\theta, \quad \delta \succ 1. \end{aligned}\right\} \tag{9}$$

where θ is the dimensionless temperature, *w* is the dimensionless velocity, ψ is the pressure gradient parameter, Pr is Prandtl number, γ is dimensionless viscosity variation parameter, δ is the difference between the two radii (gap), $Gr = \frac{g\beta\left(T_0 - T_a\right)r_0^2}{U\mu_0}$ is the grashof number and $Br = \frac{U^2\mu_0}{k\left(T_0 - T_a\right)}$ is the Brinkmann number, $Bi = \frac{r_0 h}{k}$ is the Biot number.

It is important to note that if $b = 0$, this implies Poisselle flow and if $b > 0$, this implies generalized Couette flow.

The set of equations (7)–(8) under the boundary conditions (9) were solved numerically by applying the shooting technique together with a fourth-order Runge-Kutta-Fehlberg integration scheme [12]. The temperature and the velocity obtained were utilized to find the skin-friction coefficient (C_f) and the Nusselt number (*Nu)* given as:

$$C_f = \frac{r_0\tau_w}{U\mu_0} = e^{-\gamma\theta}\left.\frac{dw}{d\eta}\right|_{\eta=1,\delta}, \ Nu = \frac{r_0 q_w}{k\left(T_0 - T_a\right)} = -\left.\frac{d\theta}{d\eta}\right|_{\eta=1,\delta}. \tag{10}$$

3. ENTROPY ANALYSIS

In convection process, irreversibility arises due to the heat transfer and the viscous effect of the fluid and

this causes entropy generation. Following Mahmud and Fraser [13], the local volumetric rate of entropy generation for a viscous incompressible fluid is defined as:

$$E_G = \frac{k}{T_0^2}\left(\frac{dT}{dr}\right)^2 + \frac{\mu(T)}{T_0}\left(\frac{du}{dr}\right)^2. \quad (11)$$

It is clear from equation (11) that two sources are responsible for entropy generation. The first term on the right hand side of equation (11) is irreversibility due to heat transfer while the second term represents irreversibility due to fluid friction. Introducing equation (6) into equation (11), we obtain the dimensionless form of local entropy generation rate as:

$$Ns = \frac{T_0^2 E_G r_0^2}{k\left(T_0 - T_a\right)^2} = \left(\frac{d\theta}{d\eta}\right)^2 + \frac{Bre^{-\gamma\theta}}{\Omega}\left(\frac{dw}{d\eta}\right)^2 \quad (12)$$

where $\Omega = (T_0 - T_a)/T_a$ is the temperature difference parameter and *Br* = *EcPr* is the Brinkmann number. The Bejan number *Be* is define as

$$Be = \frac{N_1}{N_s} = \frac{1}{1+\Phi} \quad (13)$$

where $N_s = N_1 + N_2$,

$N_1 = \left(\frac{d\theta}{d\eta}\right)^2$ (Irreversibility due to heat transfer),

$N_2 = \frac{Bre^{-\gamma\theta}}{\Omega}\left(\frac{dw}{d\eta}\right)^2$ (Irreversibility due to fluid friction),

$\Phi = \frac{N_2}{N_1}$ (Irreversibility ratio).

The Bejan number (Be) as shown in equation (13) has a close bounded range between 0 and 1. Irreversibility due to heat transfer is dominated if the Bejan number is one while irreversibility due to fluid friction is dominated if the Bejan number is zero. Both irreversibility due to heat transfer and fluid friction contribute equally if the Bejan number is half.

4. RESULTS AND DISCUSSION

A set of selected graphical results are presented in the figures below in order to study the influence of all parameters contained in the present flow problem.

5. VELOCITY AND TEMPERATURE PROFILE

The effect of parameter variations on the velocity profiles are presented in Figures **2-7**. In Figure **2** as the pressure gradient (ψ) is increasing, it is noticed that the velocity profile between the two concentric pipes is increasing. In Figure **3**, the velocity profile increases as the Grashof number (Gr) is increasing. Similarly, in Figures **4, 5** and **6**, it is noticed that as each of the parameters, Prandtl number (Pr), wall parameter (b) and viscosity variation parameter (γ) are increasing, the velocity profiles are increasing as well. Figure **7** depicts that increase in Biot number (Bi). As Bi is increasing, we noticed decrease in the velocity profile. Generally, it is noticed that increase in all the parameters mentioned above have no effect on the inner and outer cylindrical pipes but increase in wall parameter increase the velocity of the outer cylinder. The effect of parameter variations on the temperature profiles are presented in Figures **8-13**. Here it is noticed that as each of the parameters $\psi, Gr, \Pr,$ and b are increasing, the temperature profiles are increasing. But with increase in γ and Bi tend to decrease the temperature profiles.

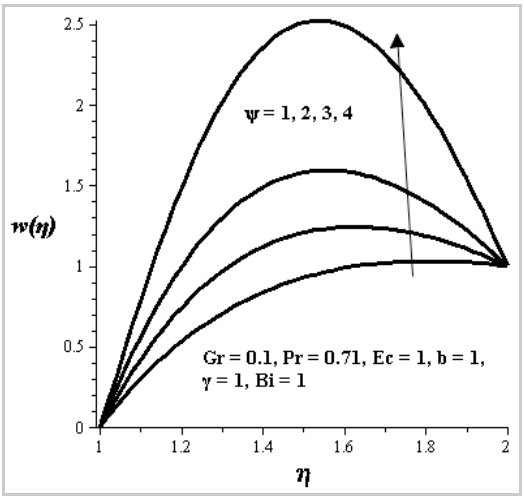

Figure 2: Effect of increasing pressure gradient on velocity profile.

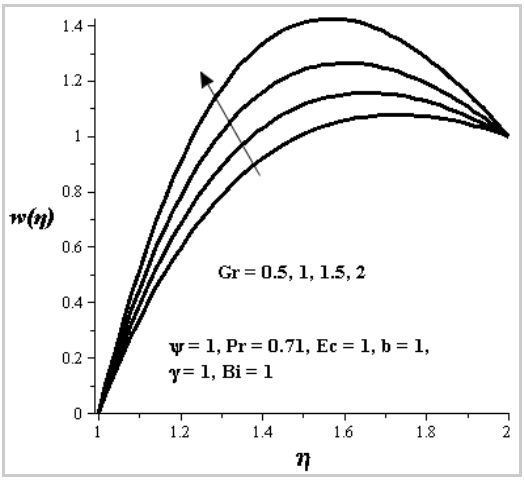

Figure 3: Effect of increasing grasholf number on velocity profile.

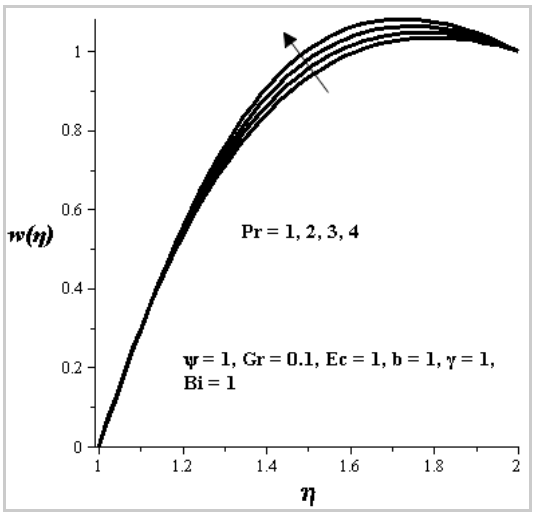

Figure 4: Effect of increasing prandlt number on velocity profile.

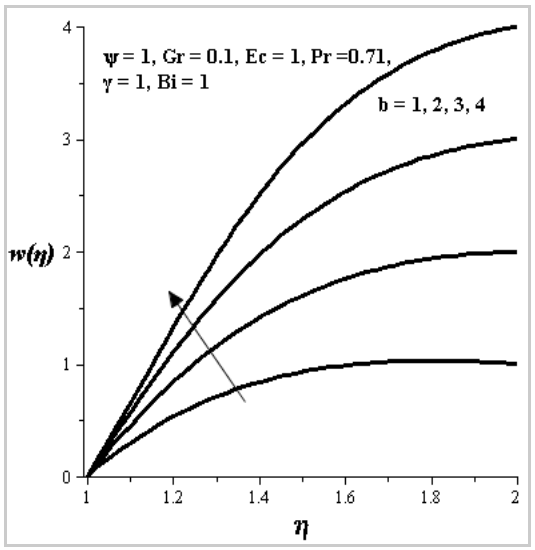

Figure 5: Effect of increasing wall parameter on velocity profile.

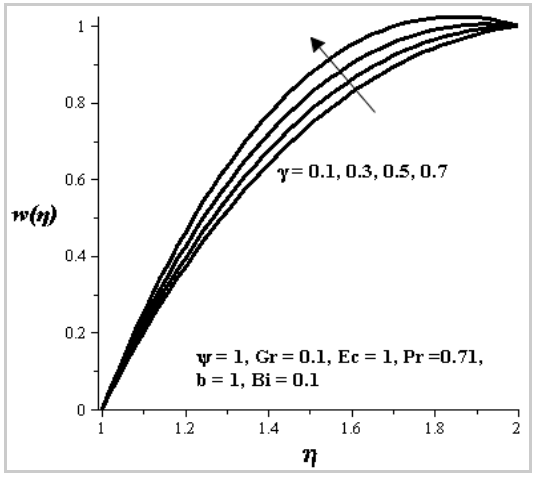

Figure 6: Effect of increasing viscosity variation parameter on velocity profile.

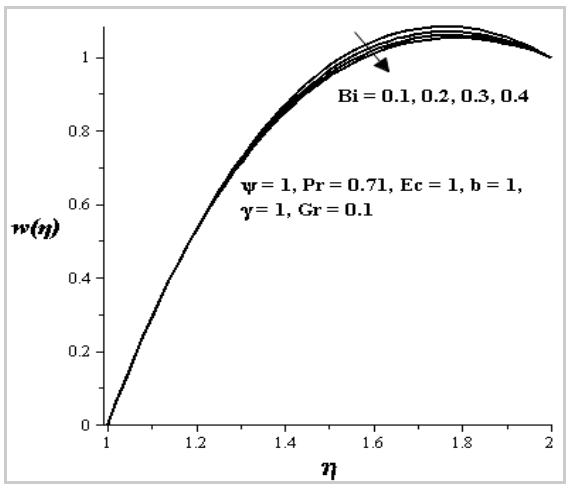

Figure 7: Effect of increasing biot number on velocity profile.

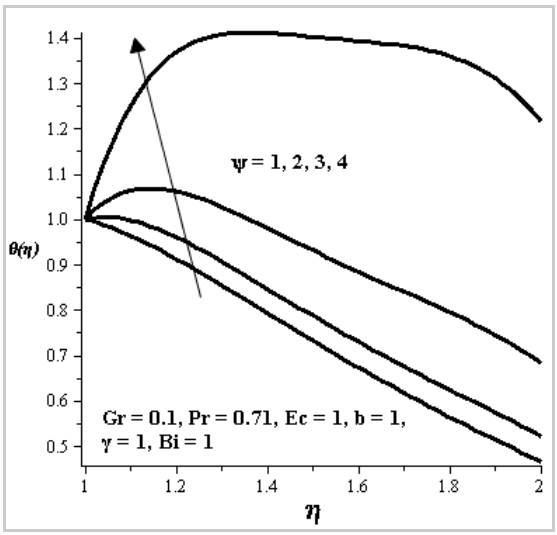

Figure 8: Effect of increasing pressure gradient on temperature profile.

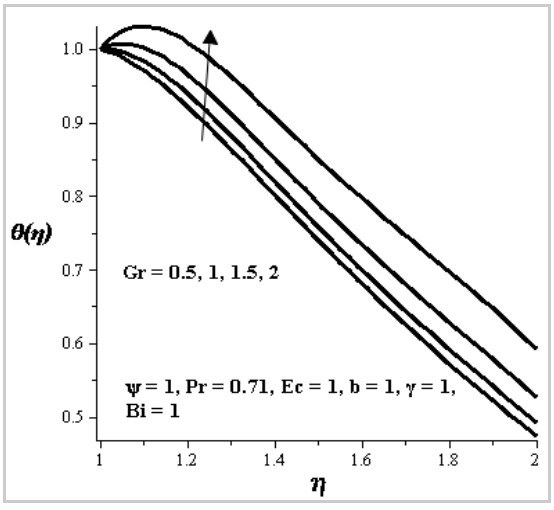

Figure 9: Effect of increasing grashof number on temperature profile.

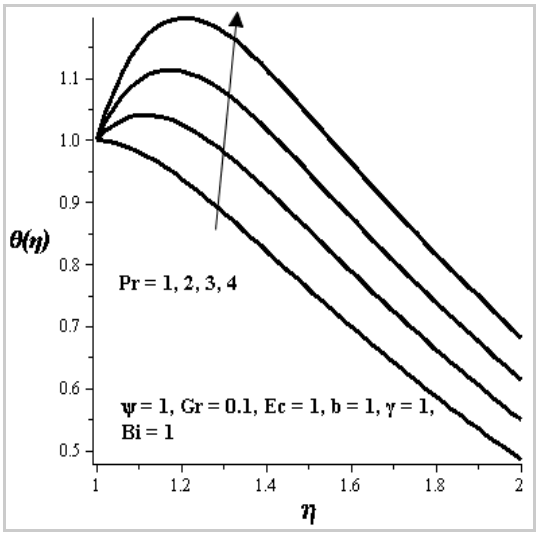

Figure 10: Effect of increasing prandtl number on Temperature profile.

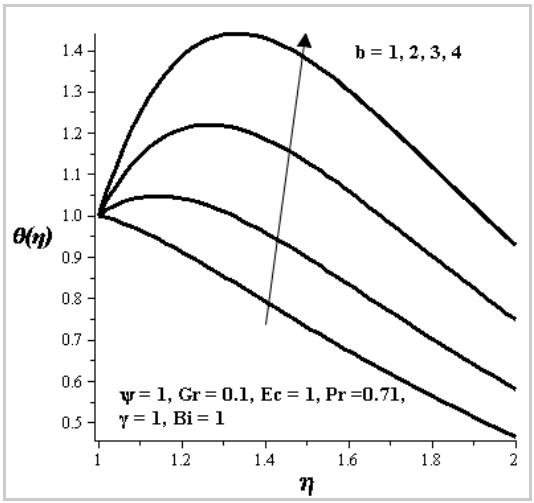

Figure 11: Effect of increasing wall parameter on Temperature profile.

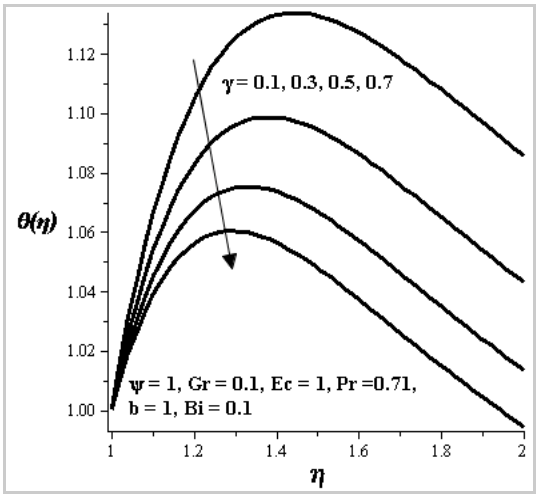

Figure 12: Effect of increasing viscosity variation parameter on Temperature profile.

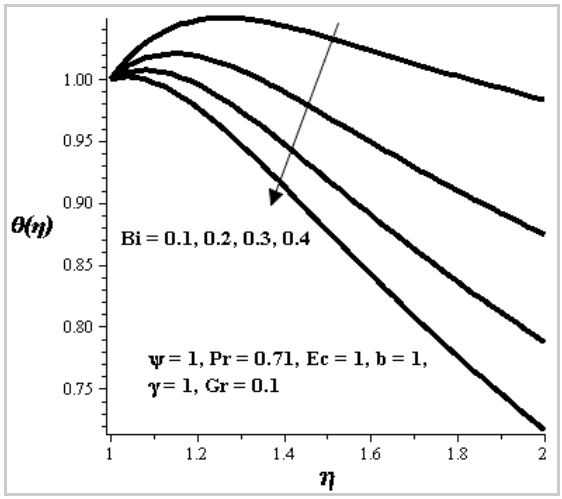

Figure 13: Effect of increasing Biot number on Temperature profile.

6. SKIN FRICTION AND NUSSELT NUMBER

The effects of the variation parameters on the skin friction and nusselt number are illustrated in Figures (**14-17**). Figure **14** shows that the skin friction increases at the inner cylinder and decreases at the outer cylinder with increase in the pressure gardient versus viscosity variation parameter. Figure **15** shows the effect of increasing pressure gradient versus Biot number on the skin friction. As these two parameters are increasing, the skin friction at the inner increases while at the oute r decreases. The effect of increasing pressure gradient (ψ) versus Grashof number (Gr) is depicted in Figure **16**. As ψ and Gr are increasing, it is noticed that Nusselt number decreases at inner cylinder and increase at outer cylinder. Similarly, Figure **17** illustrates the effect of increasing ψ and γ. Increase in these two parameters, decreases the nusselt number at inner cylinder and increases the nusselt number at outer cylinder.

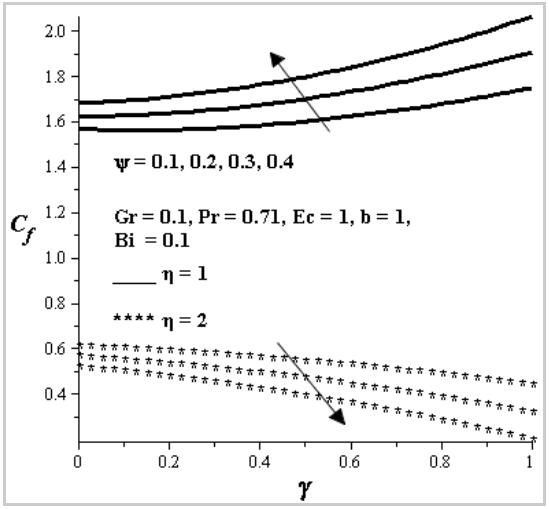

Figure 14: Effect of increasing pressure gradient versus viscosity variation parameter on skin friction.

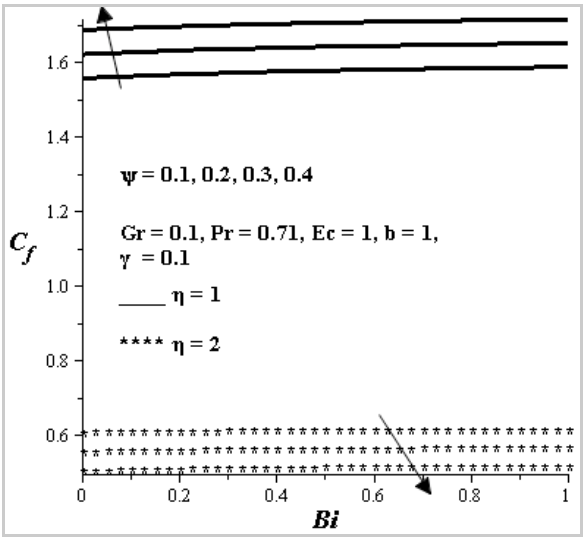

Figure 15: Effect of increasing pressure gradient versus Biot number on skin friction.

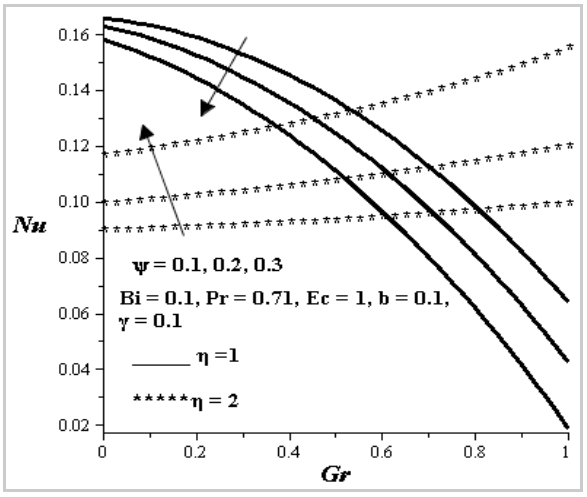

Figure 16: Nusselt number with increasing in pressure gradient versus Grashof number.

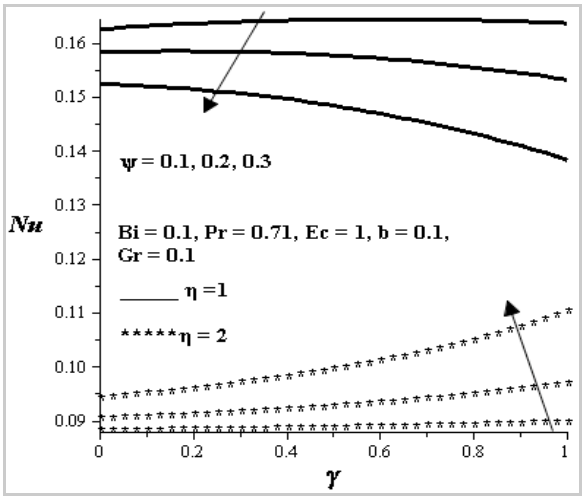

Figure 17: Nusselt number with increasing in pressure gradient versus viscosity variation parameter.

7. ENTROPY GENERATION RATE

Various effects of the flow parameters on entropy generation rate are shown in Figures (**18-22**). The effect of increasing pressure gradient on entropy generation rate is shown in Figure **18**. As ψ is increasing, there is an increase in the entropy generation rate at both cylinder and decrease in entropy generation rate between them. The increase is well pronounced at the inner cylinder. Figures (**19-21**) show the effects of increasing Gr, group parameter $\left(Br\Omega^{-1}\right)$ and b. As each of these parameters is increasing, we noticed increase in the entropy generation at the inner cylinder with no effect on the outer cylinder. In Figure **22**, the effect of Bi on the entropy generation rate is depicted. An increase in Bi, increase the entropy generation rate across the flow.

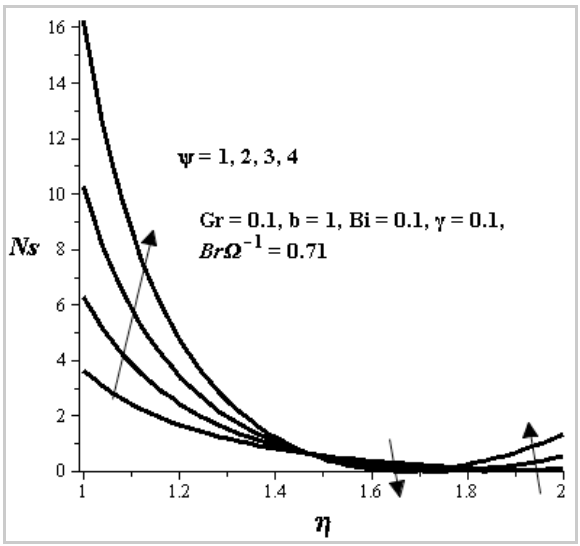

Figure 18: Effect of increasing pressure gradienr on entropy generation.

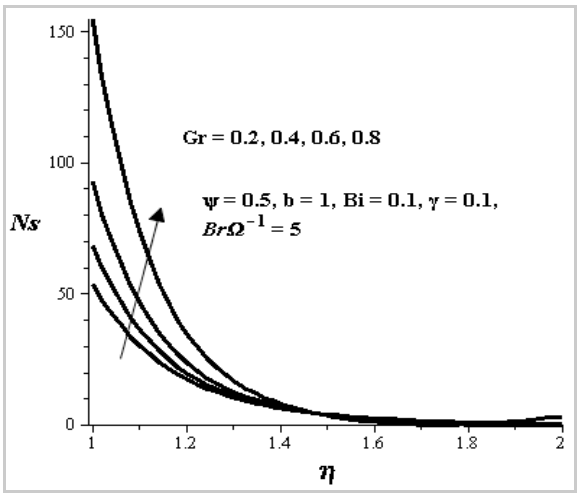

Figure 19: Effect of increasing Grashof number on entropy generation.

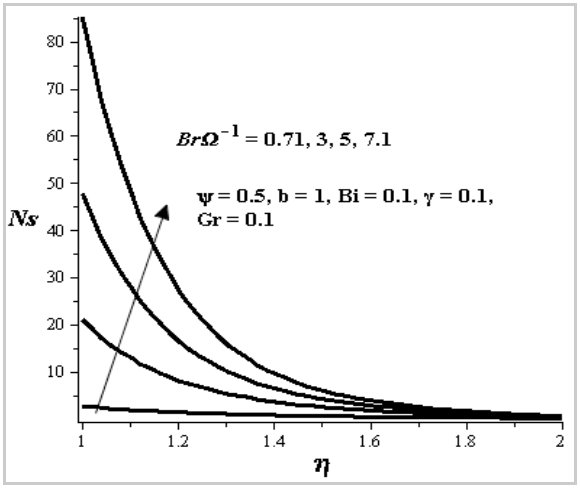

Figure 20: Effect of increasing group parameter on entropy generation.

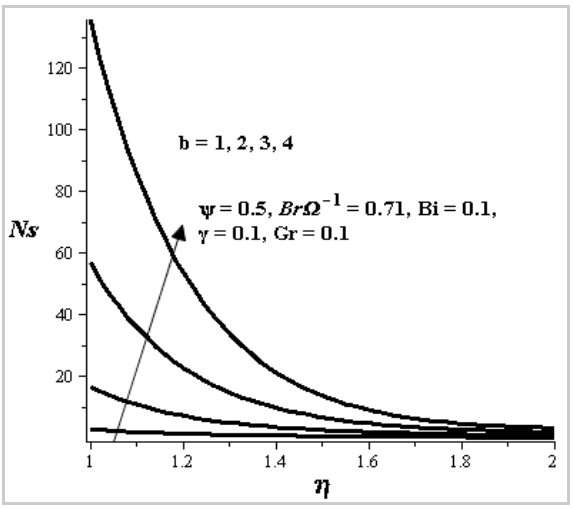

Figure 21: Effect of increasing wall parameter on entropy generation.

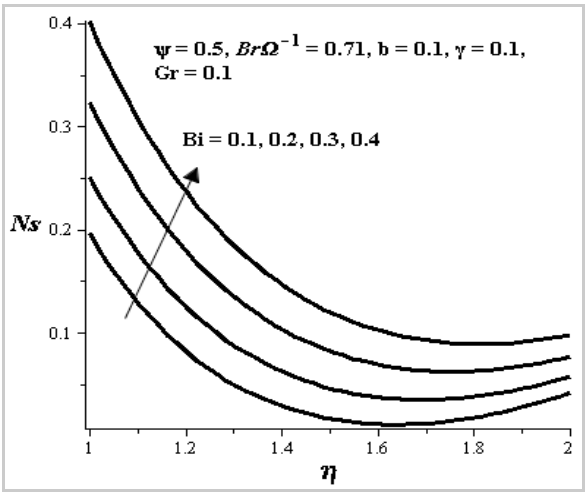

Figure 22: Effect of increasing Biot number on entropy generation.

8. THE BEJAN NUMBER

Figures (**23-27**) illustrate the effect of flow parameters variation on the Bejan number. Figures **23** and **24** show the effect of increasing ψ and Gr. It is noticed that the Bejan number decreases as each of these parameters is increasing. Thus, fluid friction irreversibility dominates at both cylinder. Figures **25** and **27** illustrate the effect of increasing group parameter and Biot number. An increase in each of these parameters, increase the Bejan number at both cylinder. This indicate that irreversibility due to heat transfer dominate both cylinder. In Figure **26**, the effect of increasing in wall parameter on the Bejan nunber is illustrated. As wall parameter is increasing, it is noticed that the Bejan number at the inner cylinder has no effect. Between the inner and outer, there exist decrease in the Bejan number and at the outer cylinder, the Bejan number increases. This signify that the irreversibility due to fluid friction dominate between the cylinder and irreversibility due to heat transfer dominate at the outer cylinder.

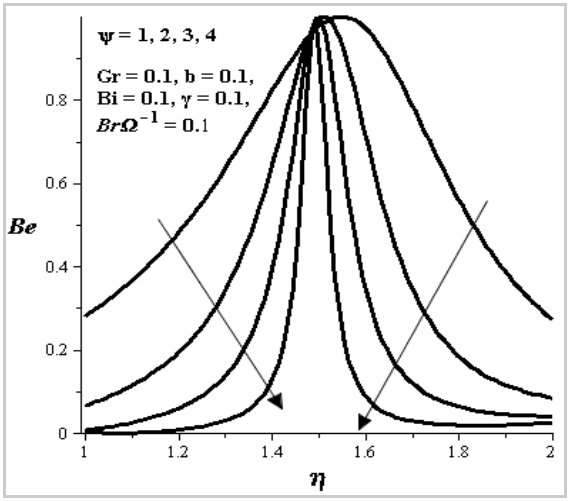

Figure 23: Effect of pressure gradient on the bejan number.

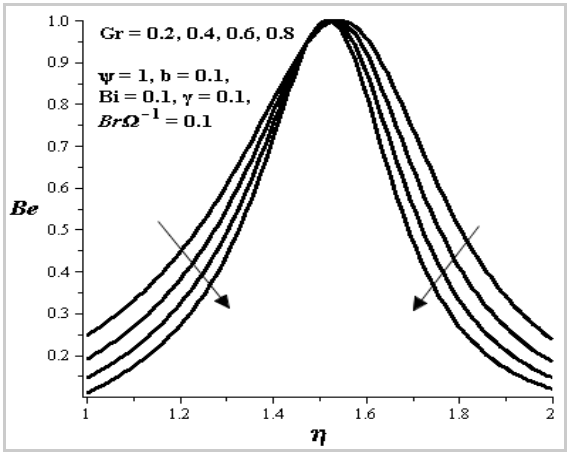

Figure 24: Effect of grashof number on the bejan number.

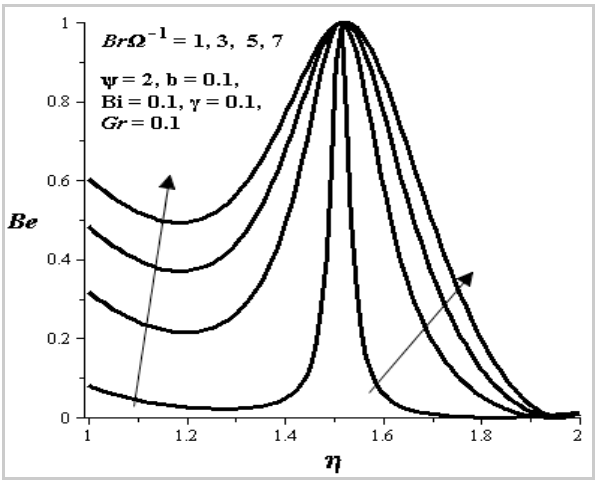

Figure 25: Effect of group parameter on the bejan number.

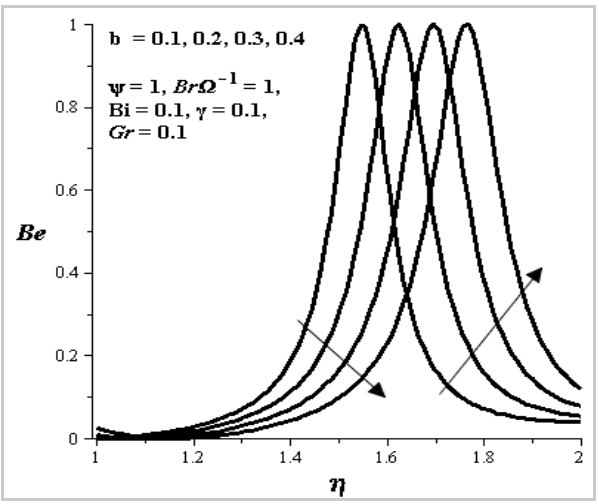

Figure 26: Effect of wall parameter on the bejan number.

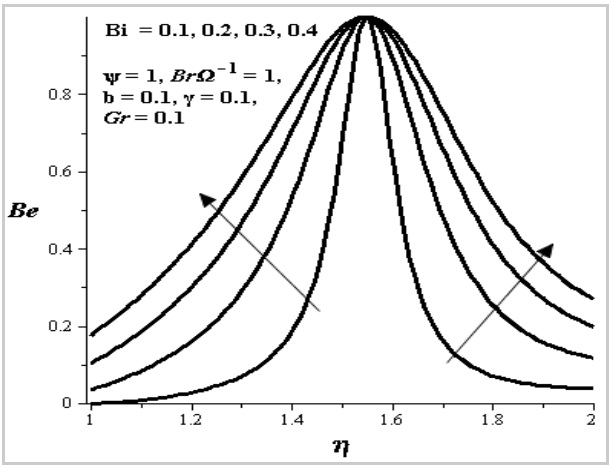

Figure 27: Effect of biot number on the bejan number.

9. CONCLUSION

In this paper, we have theoretically investigated the steady flow of an incompressible viscous fluid between two concentric cylindrical pipes in a generalized Couette flow together with the buoyancy effects. Some of the results obtained can be summarized as follows;

1. The velocity profile increases as $\psi, \Pr, Gr, b$ and γ are increasing while the velocity profile decrease with increase in Bi.

2. The temperature profile increases as $\psi, \Pr, Gr$ and b are increasing while it decreases with an increase in γ and Bi.

3. The skin friction increases with increase in ψ versus γ and ψ versus Bi at $\eta = 1$ while it decreases with increase in ψ versus γ and ψ versus Bi at $\eta = 2$.

4. The Nusselt number decreases with increase in ψ versus Gr and ψ versus γ at $\eta = 1$ while it increases with increase in ψ versus Gr and ψ versus γ at $\eta = 2$.

5. The entropy generation rate increases at inner cylinder with increase in $Gr, Br\Omega^{-1}$ and b with little or no effect on outer cylinder. But with increase in Bi, the entropy generation rate increases across the flow.

6. The Bejan number decreases with an increase in Gr and ψ. It increases with an increase in $Br\Omega^{-1}$ and Bi.

NOMENCLATURE

u	Axial velocity $[ms^{-1}]$.
k	Thermal conductivity $[W/mK]$.
U	Mean velocity $[ms^{-1}]$.
P	Fluid pressure $[Nm^{-2}]$.
T	Fluid temperature [K].
E_G	Entropy generation $[W/m^3K]$.
Be	Bejan number [-]
Ub	Outer wall velocity $[ms^{-1}]$.
T_a	Ambient temperature [K].
T_0	Inner cylinder temperature [K].
b	Wall parameter.
z	Axial distance [m].

g	Acceleration due to gravity $[ms^{-2}]$.
Pr	Prandtl number.
Br	Brinkmann number.
Ec	Eckert number.
h	Heat transfer Coefficient $[W/m^2K]$.
w	Dimensionless velocity.
Nu	Nusselt number.
Bi	Biot number.
r_0, r_1	Inner and outer radii [m].
m	Viscosity variation parameter.
C_f	Skin-friction coefficient.
Gr	Grashof number.
N_s	Dimensionless form of entropy generation.

Greek Symbols

θ	Dimensionless temperature.
Φ	Irreversibility ratio.
η	Dimensionless radius.
γ	Dimensionless viscosity variation parameter.
ψ	Pressure gradient.
Ω	Temperature difference parameter.
σ	Difference between two radii.

REFERENCES

[1] Makinde OD, Franks O. On MHD unsteady reactive Couette flow with heat transfer and variable properties. Central European Journal of Engineering 2014; 4(1): 54-63. http://dx.doi.org/10.2478/s13531-013-0139-0

[2] Attia HA, Sayed-Ahmed ME. Unsteady hydromagnetic generalized Couette flow of a non-Newtonian fluid with heat transfer between parallel porous plates. Heat Transfer 2008; 130(11): 11454-1. http://dx.doi.org/10.1115/1.2927392

[3] Theuri D, Makinde OD. Thermodynamic analysis of variable viscosity MHD unsteady generalized Couette flow with permeable walls: Applied and Computational Mathematics 2014; 3(1): 1-8. http://dx.doi.org/10.11648/j.acm.20140301.11

[4] Asghara S, Ahmada A. Unsteady Couette flow of viscous fluid under a non-uniform magnetic field. Applied Mathematics Letter 2012; 25: 1953-1954. http://dx.doi.org/10.1016/j.aml.2012.03.008

[5] Chinyoka T, Makinde OD. Analysis of transient generalized Couette flow of a reactive variable viscosity third-grade liquid with asymmetric convective cooling. Mathematical and Computer Modelling 2011; 54: 160-174. http://dx.doi.org/10.1016/j.mcm.2011.01.047

[6] Eegunjobi AS, Makinde OD. Entropy generation analysis in transient variable viscosity Couette flow between two concentric pipes. Journal of Thermal Science and Technology 2014; 9(2): JTST 0008.

[7] Liua Y, Zhenga L, Zhang X. Unsteady MHD Couette flow of a generalized Oldroyd-B fluid with fractional derivative. Computer and Mathematics with Application 2011; 61: 443-453. http://dx.doi.org/10.1016/j.camwa.2010.11.021

[8] Asghar S, Hayat T and Ariel PD. Unsteady Couette flows in a second grade fluid with variable material properties. Communications in Nonlinear Science and Numerical Simulation 2009; 14: 154-159. http://dx.doi.org/10.1016/j.cnsns.2007.07.016

[9] Dou HS, Khoo BC, Yeo KS. Instability of Taylor-Couette flow between concentric rotating cylinders. International Journal of Thermal Sciences 2008; 47: 1422-1435. http://dx.doi.org/10.1016/j.ijthermalsci.2007.12.012

[10] Hashemabadi SH, Mirnajafizadeh SM. Analysis of viscoelastic fluid flow with temperature dependent properties in plane Couette flow and thin annuli. Applied Mathematical Modelling 2010; 34: 919-930. http://dx.doi.org/10.1016/j.apm.2009.07.001

[11] Agrawal A, Prabhu SV. Deduction of slip coefficient in slip and transition regimes from existing cylindrical Couette flow data. Experimental Thermal and Fluid Science 2008; 32: 991-996. http://dx.doi.org/10.1016/j.expthermflusci.2007.11.010

[12] Nachtshein PR and Swigert P. Satisfaction of the asymptotic boundary conditions numerical solution of the system of nonlinear equation of boundary layer type. NASA TND-3004 1965.

[13] Mahmud S and Fraser RA. Flow, thermal and entropy generation characteristic inside a porous channel with viscous dissipation. Int J Therm Sci 2005; 44: 21-32. http://dx.doi.org/10.1016/j.ijthermalsci.2004.05.001

Received on 11-04-2015 Accepted on 12-30-2015 Published on 13-07-2016

DOI: http://dx.doi.org/10.15377/2409-5826.2016.03.01.3